Quantum computation using electrons trapped by surface acoustic waves

C. H. W. Barnes, J. M. Shilton, and A. M. Robinson
Cavendish Laboratory, University of Cambridge, Madingley Road, Cambridge CB3 0HE, United Kingdom
(Received 24 January 2000)

We describe in detail a set of ideas for implementing qubits, quantum gates, and quantum gate networks in a semiconductor heterostructure device. Our proposal is based on an extension of the technology used for surface acoustic wave (SAW) based single-electron transport devices. These devices allow single electrons to be captured from a two-dimensional electron gas in the potential minima of a SAW. We discuss how this technology can be adapted to allow the capture of electrons in pure spin states and how both single and two-qubit gates can be constructed using magnetic and nonmagnetic gate technology. We give designs for readout gates to allow the spin state of the electrons to be measured and discuss how combinations of gates can be connected to make multiqubit networks. Finally we consider decoherence and other sources of error, and how they can be minimized for our design.

I. INTRODUCTION

The quantum mechanics of interacting many-particle systems presents an intractable problem for classical computers. The vast Hilbert space and the correlation between particles prohibits the exact simulation of all but the smallest systems by classical means. Thus, by manipulating and observing even a relatively small many-particle system, a ''computation'' could be performed which no classical computer would be capable of. Such a system, together with its measuring apparatus is referred to as a ''quantum computer.''[1,2] Extensive research in this field has shown that quantum computers can be used to solve any computational problem, that is, they are capable of universal computation. However, it is clear that they are efficient at simulating quantum systems,[3–6] and fast algorithms for factoring large numbers[7] and searching databases[8–10] have been found.

Two factors considerably simplify the design of a suitable many-particle system for universal quantum computation: it is sufficient to construct only a single line of two-state systems (so called qubits) which are weakly coupled;[11–13] and it is not necessary to maintain global phase coherence throughout a computation.[14–19] These simplifications are probably outweighed by the necessity that each qubit must be individually addressable, so that its pseudospin can be independently rotated through an arbitrary angle about any two chosen ''axes,'' and by the requirement that the coupling between each pair of qubits must be accurately controllable. Useful qubits, together with suitable coupling mechanisms, can be found in almost every area of physics and chemistry and there are a growing number of attempts to demonstrate control over the rotation of and coupling between qubits.[20–37]

The proposal for quantum computation that we outline in this paper is in the semiconductor quantum dot category.[38–40] It is based on recent experiments in which a surface acoustic wave (SAW) is passed across a semiconductor heterostructure containing a two-dimensional electron gas (2DEG) and is incident on a depleted quasi-one-dimensional channel (Q1DC). In this experiment it is possible to capture a single electron from the 2DEG in each minimum of the SAW wave and transport them through the Q1DC.[41–43] Our proposal is based on the assumption that by placing a series of N Q1DC's in parallel, a SAW can be made to capture N electrons in each of its minima, with one electron in each Q1DC. A single-quantum computation would be performed by the N electrons in a single SAW minimum as they are dragged through a pattern of magnetic and nonmagnetic surface gates, which carry out single and two-qubit operations. At the end of the computation the electrons would then be channeled into a set of N readout gates that would determine the final spin state of each electron. Each SAW minimum would contain an identical number of electrons prepared in an identical manner and would therefore perform the same computation. This would allow the readout gates to produce a measurable current representing the output of the quantum computer. Since the qubits would be carried along with the SAW, this proposal is an example of a ''flying qubit'' design.[20,44] We discuss these ideas based on using the electron spin to encode the qubits, but the idea could easily be extended to use the two states of a double quantum well, or the transverse states in laterally patterned parallel Q1DC's.

The paper is organized as follows. In Sec. II we describe the SAW-based single-electron transport experiment, and discuss how SAW's incident on a Q1DC capture electrons. We then discuss how a magnetic field would enable the electrons to be captured as qubits in prepared states. In Sec. III we show how magnetic gating can be used for single qubit operations, and how nonmagnetic gating can produce two-qubit operations. A simple model is used to detail the operation of the two-qubit gate. Section IV discusses the integration of the single and two-qubit gates to produce a C-NOT gate and larger networks of gates. Section V addresses the question of how the final state of the qubits can be read out and in Sec. VI we consider possible sources of error and decoherence.

II. PRODUCTION OF SINGLE AND MULTIPLE QUBITS

A. Production of a quantized current using SAW's

Figure 1 shows a schematic diagram of a SAW-based quantized-current device.[41–43] It consists of a GaAs/AlGaAs heterostructure with NiCr/Al interdigitated transducers pat-

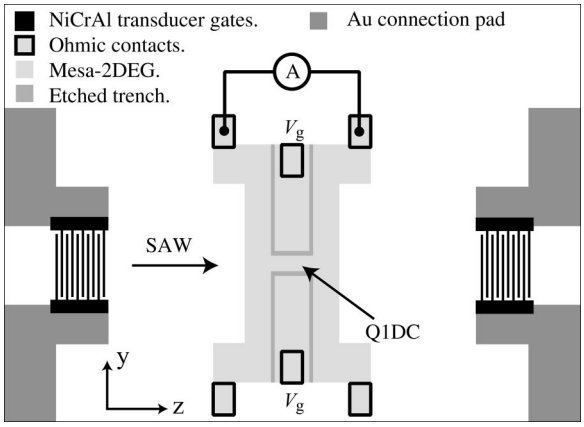

FIG. 1. Schematic diagram showing an experimental device that produces a quantized acoustoelectric current.

terned on either side of a central etch-defined mesa that contains a 2DEG. When a high frequency ac signal is applied to one of these transducers it produces a SAW, via the piezoelectric effect, which can be detected with the other transducer. As a SAW propagates across the mesa region, the traveling periodic electrostatic potential it produces drags electrons from the 2DEG along with it. For a typical SAW frequency of 3 GHz and an applied power of 10 dBm this produces a measurable current in the nanoamp range. For the quantized-current devices, the mesa is patterned so that it is split into two 2DEG regions (source and drain) connected by a narrow depleted Q1DC. The Q1DC can be formed either by surface Schottky gates, or by an etching technique developed by Kristensen *et al.*[45,46] as shown in Fig 1. It has been shown experimentally[41–43] that over certain ranges of SAW power and gate voltage, the current that is produced by the SAW becomes quantized in units of ef, where e is the elementary electronic charge and f is the SAW frequency. The lowest quantized value observed represents the transport of a single electron from the source to the drain reservoir in each SAW minimum through the Q1DC. The electrons travel through the Q1DC with a mean speed equal to the SAW velocity, which is 2700 ms^{-1} on the (001) plane of GaAs. Recent experimental results have demonstrated this effect with an accuracy of five parts in 10.[4,47]

B. Discussion of capture process

At present, there is only an incomplete understanding of the mechanism by which electrons are captured and transported by the SAW through the Q1DC.[48–52] This capture process is intrinsically time dependent; it involves the Coulomb interaction between many particles; and includes quantum-mechanical confinement, tunneling, and decoherence.

Figures 2(a) and 2(b) show a contour plot of the effective potential in the Q1DC connecting the source and drain 2DEG's, and a cross section through the same potential. Both figures are schematic and shaded regions indicate electron occupation. These figures illustrate that as a SAW minimum approaches the entrance to the Q1DC, the SAW potential trough narrows and becomes a quantum dot. The size of this quantum dot implies that, at the point that it forms, it will be occupied by many electrons. As it shrinks in passing

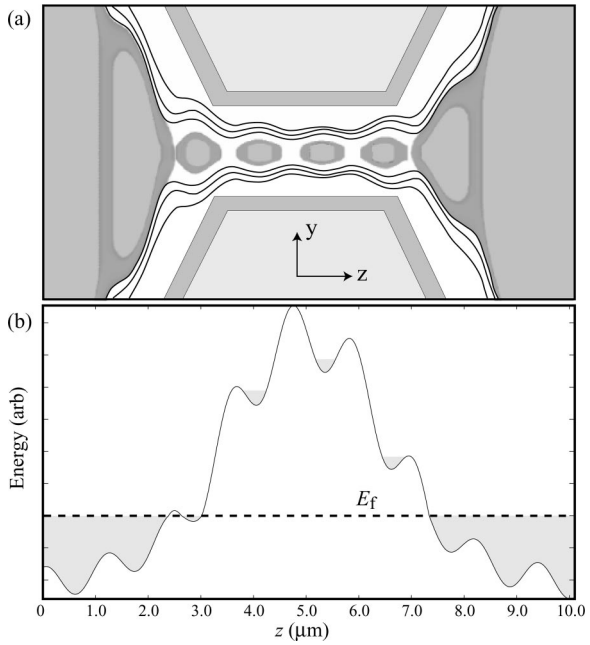

FIG. 2. (a) Schematic diagram showing the effective potential due to a SAW passing across a Q1DC; (b) potential through the center of (a), parallel to the Q1DC. Shaded regions in (a) and (b) indicate electron occupation.

through the Q1DC, electrons will be forced out. Electrons that are left in the dot are taken far from equilibrium with the source and drain reservoirs as they pass across the Q1DC. The distances and barrier heights between adjacent quantum dots are sufficiently large that the dots in the Q1DC can be considered to be independent as far as quantum-mechanical tunneling is concerned.

From a classical perspective, the electrons that are most likely to be captured and transported through the Q1DC by the SAW will be those that are least energetic in the rest frame of the SAW. Quantum mechanically, the SAW minima will contain electrons in localized states and the SAW would not be expected to eject these electrons in favor of capturing those in higher-energy states. This is born out by classical simulations and by evaluations of the 1D single-particle time-dependent Schrödinger equation.[52] Figure 3 il-

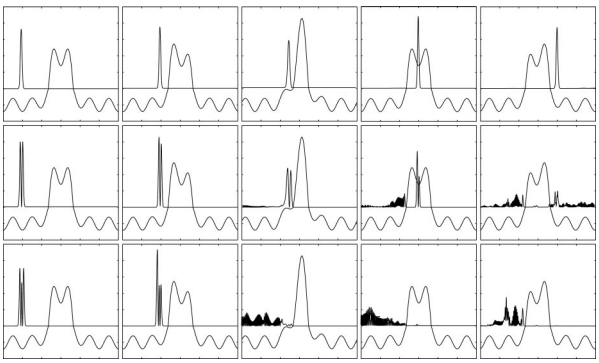

FIG. 3. Time-dependent solutions to 1D single-particle Schrödinger equation for the first three states of a particular SAW minimum. The squared moduli of the wave functions as a function of z are shown together with the effective potential. The time sequence is from left to right.

lustrates the quantum-mechanical capture process by showing the evolution of the wave functions of the first three bound states of a SAW minimum as it approaches and then passes through a Q1DC. The potential in Fig. 3 was chosen so that the mean current would correspond to the transport of 1.5 electrons per cycle. It can be seen in the upper sequence that the lowest state is simply carried along with the traveling SAW, even through the Q1DC. However, the second state is partially reflected as it arrives at the Q1DC, and the third state is completely rejected. All higher-energy states, including those that are delocalized in the bulk 2DEG region, are also reflected.

The effect of the Coulomb interaction is important in the capture process because as quantum dots form and are brought to the Fermi energy, the screening between their trapped electrons is reduced. Once above the Fermi energy, this screening appears only as an image charge in the 2DEG. The Coulomb interaction will therefore control the form of the time-dependent wave functions, the state energies, and ultimately the number of electrons left in a dot as it passes through the Q1DC.

Quantum-mechanical decoherence is relevant to the capture and escape processes because it determines whether there is an integer number of electrons trapped in the dot or not, and it affects the quantum states of these electrons. If at some instant the energy of one of the electrons in a particular dot is too large for it to be contained by that dot—or large enough that tunneling becomes important—then the wave function of this electron will start to leak out of that dot. An electron that is in the process of leaving will initially propagate over the adjacent 2DEG maintaining coherence with the electrons left in the dot and will then lose this coherence as it interacts with conduction electrons. The decoherence will determine whether the electron leaves and will cause the dot to be left in a mixed state. As more and more electrons escape it is probable that the density matrix of the dot will become increasingly diagonal. For the case where finally only a single electron remains in the dot this would mean that its density matrix would simply be a half and half mixture of spin up and spin down. Such a mixed state is not suitable for quantum computation.

C. Pure states

For quantum computation it is necessary to provide electrons in pure states and this can be achieved by applying an external magnetic field to our device. The simple application of an external magnetic field to an N particle mixed state does not cause it to become a pure state unless it has time to relax by emitting phonons or photons: the field merely precesses the spin of each electron. However, it has a significant effect on which electrons are captured from the 2DEG by the SAW.[52] The application of an external magnetic field polarizes the electrons in the source 2DEG so that the low-energy electrons all have the same spin. The Lande g factor in GaAs is 0.44 and the amplitude of the SAW electrostatic potential is estimated from experiments to be approximately 1 meV.[41–43] Therefore, the application of a magnetic field with strength ~ 1 T would ensure that all electrons captured would have the same spin. This is illustrated schematically in Fig. 4. Once the split-gate voltage is increased to the point where only one electron is captured per cycle, these electrons will be in pure spin states even though their orbital motion may be mixed. These electrons can therefore be used as spin qubits.

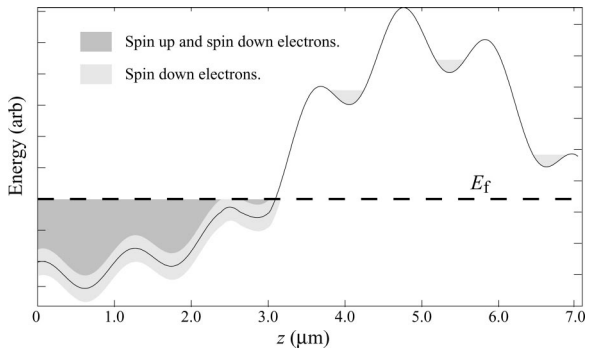

FIG. 4. Schematic diagram showing the spin up and spin down occupations of the 1D SAW potential in a finite magnetic field.

In principle a large number of such qubits may be prepared simultaneously using this method by patterning large numbers of parallel Q1DC's with surface gates[53] or by etching.

III. QUBIT GATE OPERATIONS

A quantum circuit consists of devices performing two kinds of operation on qubits. The first, the single qubit operation, acts to rotate the spin of a single qubit about an arbitrary direction in space. The second, the two-qubit operation, entangles the spin-wave functions of two adjacent qubits by altering the exchange coupling between them. A gate that produces such entanglement and is easy to produce within our scheme is the ''square root of swap'' gate.[38–40]

A. Single qubit gate

We can perform a single qubit operation on a SAW spin qubit by having it pass through the magnetic field from a local static magnet. During the time a qubit is in the field, its wave function will evolve according to the Zeeman term in Schrödinger's equation

$$\begin{bmatrix} S_z & S_x - iS_y \\ S_x + iS_y & -S_z \end{bmatrix} \begin{bmatrix} \alpha \\ \beta \end{bmatrix} = i \frac{\partial}{\partial t} \begin{bmatrix} \alpha \\ \beta \end{bmatrix}, \tag{1}$$

where $S_{x,y,z} = g\mu_B B_{x,y,z}/2$ and the qubit wave function has the form;

$$|\psi\rangle = \alpha|\uparrow\rangle + \beta|\downarrow\rangle. \tag{2}$$

For a constant external magnetic field this evolution is a precession of the qubit spin about the direction of the field.

In principle, a local static magnet with a magnetic field that points in an arbitrary direction can be provided by a magnetic force microscope or by controlled ion-beam deposition of a ferromagnetic material. However, for universal computation it is only necessary to make single qubit rotations about two independent axes and therefore it is sufficient to provide local magnetic fields that point in two orthogonal directions. As we have mentioned above, in order to provide pure states for the input, the device must be placed in an external field. This field may be used for one of the directions, and could be screened in regions where it is not needed

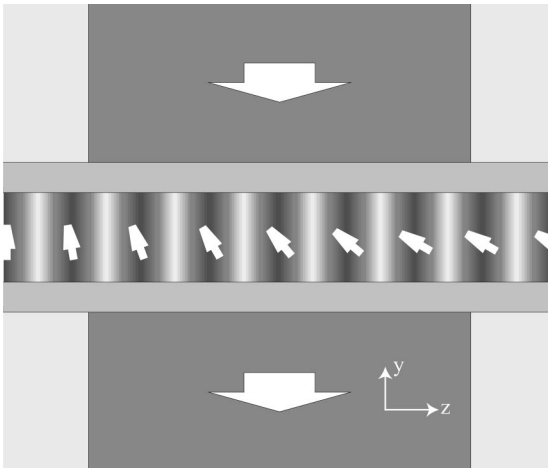

FIG. 5. Schematic diagram showing a magnetic split gate for performing a single-qubit operation. Arrows indicate the direction of the magnetization of the split gates.

by a superconducting material such as niobium. The magnetic field for the other direction can be provided by a local magnetic split gate such as that shown in Fig. 5. If this is fabricated as a split ring, then stray fields will be reduced. A material such as permalloy could be used since it has a large surface magnetization (~ 1 T) and exhibits shape anisotropy,[54] which can be exploited in setting the direction of the magnetization. If the application of a global external magnetic field proved to be inconvenient for a particular circuit design, the input magnetic field and both directions of magnetic field for single qubit operations could be provided by magnetic surface gates.

Figures 6(a) and 6(b) show how a qubit spin will precess as it passes through a magnetic split gate. They are calculated from the Zeeman contribution to the time-dependent Schrödinger equation [Eq. (1)]. For these figures, a constant field B_z has been applied and a local field B_y is switched on for a short time, representing the passage of a qubit through a magnetic split gate. In the regions where $B_y = 0$, the external field B_z causes the spin to precess around the z axis without altering its component in this direction, so that $|\alpha/\beta|^2 = \text{const}$. In the region where $B_y \neq 0$ this ratio oscillates at the Rabi frequency. These figures show that it is possible to shift the phase of the qubit components independently by altering the length of channel exposed to the external constant field, and to vary the relative amplitudes of the qubit components by varying the length of the magnetic gate. A surface gate of length ~ 220 nm with a surface field of ~ 1 T will produce a $\pi/2$ rotation on a passing qubit spin.

B. Two qubit gate

A two-qubit operation can be achieved with surface patterning that causes two adjacent qubits, captured in the same SAW minimum, to be forced into tunnel contact. Suitable gate patterning is shown schematically in Fig. 7. It consists of etched trenches defining an ''X shape'' with a central metallic surface gate that splits this shape into two channels when a negative bias is applied to it. The tunneling coefficient between adjacent dots is fully controllable using the bias on the central surface gate. For a low bias, the tunneling

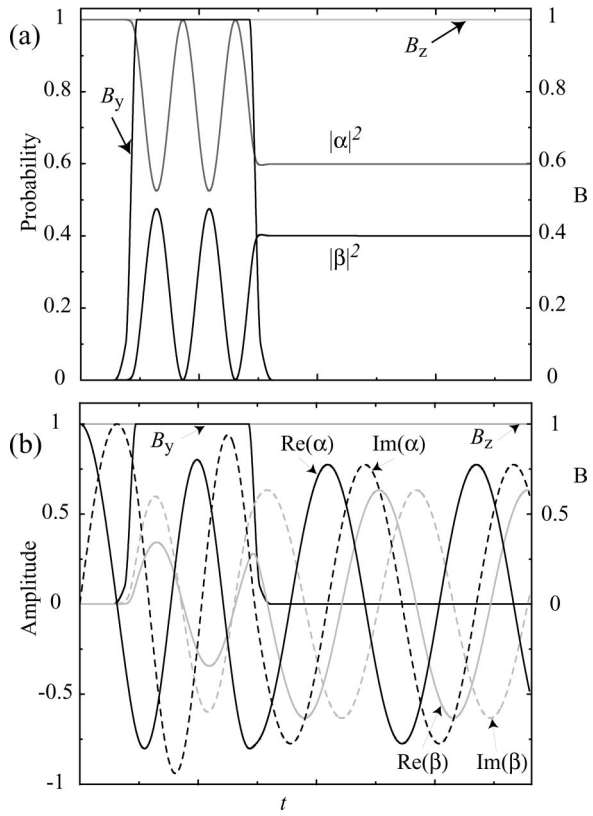

FIG. 6. (a) Magnitude of the two components of a SAW qubit as a function of time; (b) corresponding probability amplitudes as it passes through a magnetic split gate. The time dependencies of the fields B_z and B_y are indicated on the right axis.

coefficient is essentially unity, and at a large negative bias it will be zero. For a finite transmission coefficient the wave functions of the two electrons in the two dots entangle via tunneling and the Coulomb interaction and then decouple leaving just one electron in each quantum dot. This represents a two-particle unitary transformation on the initial qubit states of the trapped electrons.

C. A simple model

A number of models for a two-qubit gate made from two coupled quantum dots are given in Ref. 38. These models also apply to the two-qubit gate described above. Here, we

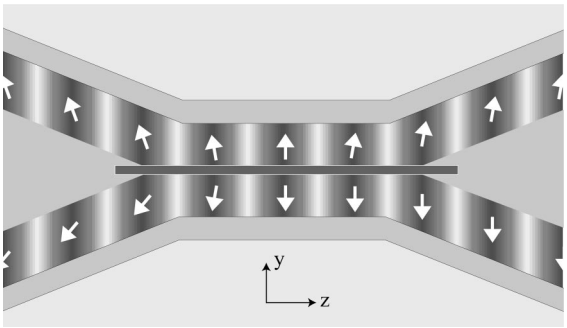

FIG. 7. Schematic diagram showing a design for a two-qubit quantum gate. Etched trenches define an ''X shape'' with controlling 2DEG's above and below and in the center there is a gold surface gate.

discuss the basic operation of this gate in terms of the Hubbard model. This model incorporates the possibility for double occupation of a single dot, which we discuss later in the section on readout gates. The electrons in the channels shown in Fig. 7 are sufficiently separated that they cannot tunnel between wells in the direction of propagation of the SAW. Away from the central tunnelling region, the wave functions in the upper and lower channels will be spin qubits of the form:

$$|\psi_u\rangle = \alpha|\uparrow\rangle + \beta|\downarrow\rangle, \tag{3}$$

$$|\psi_l\rangle = \gamma|\uparrow\rangle + \delta|\downarrow\rangle, \tag{4}$$

where $|\alpha|^2+|\beta|^2=1$ and $|\gamma|^2+|\delta|^2=1$. The indices u,l refer to the upper and lower channels, respectively. The corresponding two-particle wave function will have the form;

$$|\psi\rangle = \beta\delta|\chi_1\rangle + \alpha\gamma|\chi_2\rangle + \alpha\delta|\chi_3\rangle + \beta\gamma|\chi_4\rangle \tag{5}$$

where

$$|\chi_1\rangle = c^\dagger_{u\downarrow}c^\dagger_{l\downarrow}|0\rangle, \tag{6}$$

$$|\chi_2\rangle = c^\dagger_{u\uparrow}c^\dagger_{l\uparrow}|0\rangle, \tag{7}$$

$$|\chi_3\rangle = c^\dagger_{u\uparrow}c^\dagger_{l\downarrow}|0\rangle, \tag{8}$$

$$|\chi_4\rangle = c^\dagger_{u\downarrow}c^\dagger_{l\uparrow}|0\rangle. \tag{9}$$

The operator $c^\dagger_{i\sigma}$ creates an electron in dot i with spin σ from the empty state $|0\rangle$. In the region where the two qubits entangle, we consider two extra states that represent the possibility for double occupation of one of the dots.

$$|\chi_5\rangle = c^\dagger_{u\downarrow}c^\dagger_{u\downarrow}|0\rangle, \tag{10}$$

$$|\chi_6\rangle = c^\dagger_{l\uparrow}c^\dagger_{l\uparrow}|0\rangle. \tag{11}$$

Assuming that the electrons on each dot are tightly bound so that weak tunneling is permitted between adjacent dots in the same SAW minimum, and assuming an on-site Coulomb interaction, the time-dependent Schrödinger equation takes the form:

$$\begin{bmatrix} -2S & & & & & \\ & 2S & & & & \\ & & 0 & & \nu & \nu \\ & & & 0 & -\nu & -\nu \\ & & \nu & -\nu & U & \\ & & \nu & -\nu & & U \end{bmatrix} \begin{bmatrix} \chi_1 \\ \chi_2 \\ \chi_3 \\ \chi_4 \\ \chi_5 \\ \chi_6 \end{bmatrix} = i\frac{\partial}{\partial t} \begin{bmatrix} \chi_1 \\ \chi_2 \\ \chi_3 \\ \chi_4 \\ \chi_5 \\ \chi_6 \end{bmatrix}, \tag{12}$$

where U is the on-site Coulomb energy, S is the Zeeman energy, and ν is the single-particle tunneling energy between the two dots. The form of this Hamiltonian indicates that the states χ_1 and χ_2 evolve independently and are unaffected by the narrow tunnel barrier in the central region of the gate. This derives from the fact that two-particle tunneling between dots necessarily involves double occupation. Since the two electrons in these states have the same spin, double occupation is forbidden by the Pauli exclusion principle and therefore no tunneling can occur. This assumes that there are

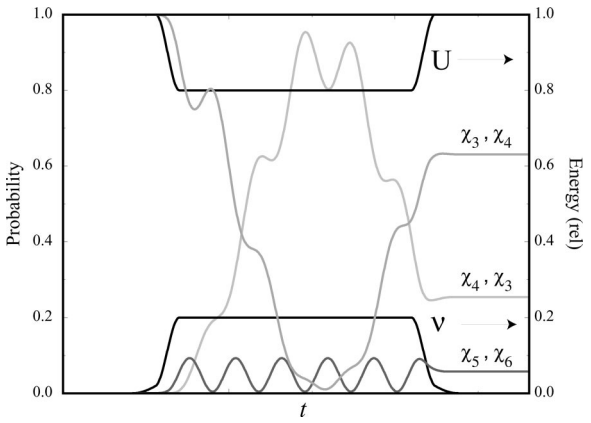

FIG. 8. Absolute values of the probability amplitudes for states $\chi_{3,\ldots,6}$ of the two-qubit gate in Fig. 7 as a function of time. The values of U and ν, right axis, are chosen to show the generic behavior of such a gate.

no other single-particle states that can be occupied. The remaining part of the Hamiltonian has four eigenvalues of the form:

$$\epsilon_1 = -J = \frac{1}{2}(U - \sqrt{U^2+16\nu^2}), \tag{13}$$

$$\epsilon_2 = 0, \tag{14}$$

$$\epsilon_3 = U, \tag{15}$$

$$\epsilon_4 = U + J = \frac{1}{2}(U + \sqrt{U^2+16\nu^2}). \tag{16}$$

For U and ν constant this implies that the dynamics of the system consist of a ''slow'' oscillation at the exchange frequency J between states χ_3 and χ_4, via the double occupation states χ_5 and χ_6, and a ''fast'' oscillation of states χ_5 and χ_6 of frequency U. Figure 8 shows a characteristic time dependence of the states $\chi_3 \cdots \chi_6$. The upper and lower traces in black show the chosen time dependence of U and ν. The lines in gray show the occupation probabilities of the states $\chi_{3,\ldots,6}$. Figure 9 shows the operation of the root of swap gate, which may be constructed from the two-qubit

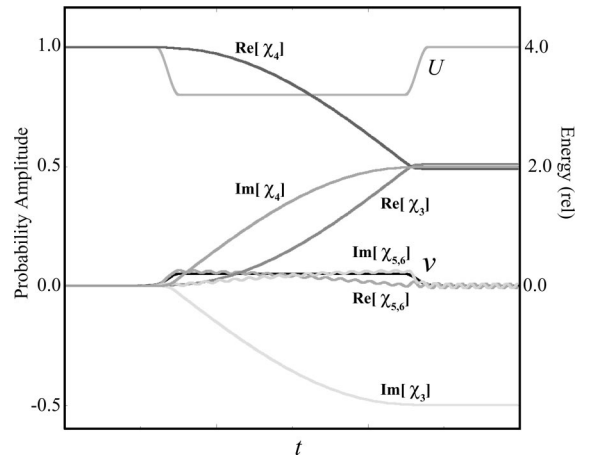

FIG. 9. Root of swap operation for two-qubit gate shown in Fig 7.

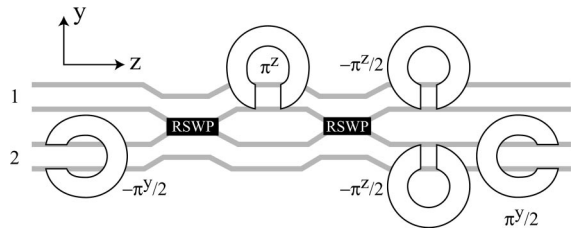

FIG. 10. Design for a C-NOT gate based on Eq. (17). Gray lines indicate etched trenches defining two parallel Q1DC's. Horse-shoe shapes represent magnetic split gates and black rectangles indicate ''root of swap'' operations.

gate (Fig. 7). Within our notation, the swap operation is a unitary operation that leaves the probability amplitudes for the first two states unchanged $\chi_{1,2}\rightarrow\chi_{1,2}$ and swaps the amplitudes of the second two states $\chi_{3,4}\rightarrow\chi_{4,3}$. Root of swap is the square root of this unitary transformation. For this figure, the Coulomb energy U has been set to be much larger than the exchange energy J and this has resulted in low-occupation probabilities for the double occupation states $\chi_{5,6}$. This is desirable for quantum computation since these states are not qubit states and their occupation results in a form of decoherence since only the qubit states are measured at the end of the computation. For $J=0.01$ meV the time for a swap operation will be approximately $\Delta t=0.2$ ns. Since the SAW travels at 2700 ms^{-1} this would correspond to a gate length $L=550$ nm. The exchange energy J depends on the tunneling probability across the central barrier region and it can therefore be set to have any value. However, using such a low value would need to be weighed against the possibility for a potential modulation of the order J in the central gate region and the necessity for the temperature to be sufficiently low. A practical design would have as large a value for J as possible, the restrictions being the smallest length of gate which could be made and the need to maximize U to prevent double occupation.

IV. QUANTUM GATE NETWORKS

A. The C-NOT gate

The single and two-qubit gates we have described constitute the only two gates necessary for the construction of universal logic in a quantum computer.[11–13] These two gates can be used to construct the quantum C-NOT operation,[38] a useful building block in quantum computer designs (e.g., see Ref. 21). In terms of our gate patterning, the C-NOT operation has the form;

$$U_{C-NOT}=\exp(i\pi S_2^y)\exp(-i\pi S_1^z/2)\exp(-i\pi S_2^z/2)U_{SW}^{1/2}\times\exp(i\pi S_1^z)U_{SW}^{1/2}\exp(-i\pi S_2^y/2). \quad (17)$$

The gate patterning necessary to produce this is shown in Fig. 10. The ''horse-shoe'' gates in the figure are used to indicate the necessity for screening stray fields from magnetic gates. This may can also be achieved by using a superconducting material such as niobium.

B. Networks

A schematic diagram of a quantum gate network is shown in Fig. 11. It consists of a large number of parallel Q1DC's.

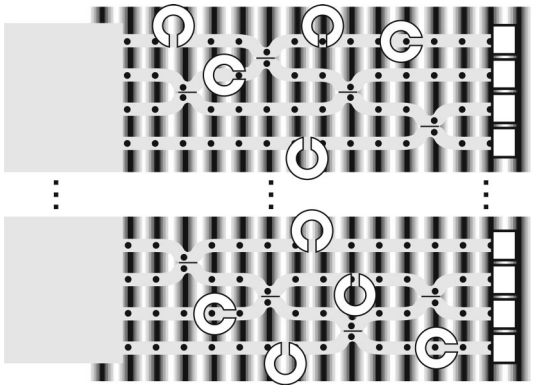

FIG. 11. Schematic diagram showing the gate pattern layout for a SAW quantum-gate network. Black and white vertical lines represent the SAW effective potential. The network of gray lines represents a set of Q1DC. Black dots represent qubits. White squares on the right-hand side represent readout gates.

Each Q1DC has single-qubit gates placed along its length and pairs of Q1DC's are coupled by two-qubit gates. Each Q1DC terminates with a readout gate. A single computation is performed by each SAW minimum as it passes across the network dragging a set of N qubits along with it. The qubits in each SAW minimum are prepared in the same way and perform the same computation. At the readout stage, each qubit passes into a separate readout gate that has two outputs arranged such that the ratio of the currents passing into them reflects the relative spin along a particular direction. The SAW performs $\sim 3.0\times 10^9$ computations per second and each calculation contributes to produce a measurable output current.

V. READOUT

Many proposals for quantum computers rely on single-electron transistors for reading the state of the output qubits.[55,31,44,36] Such techniques are also possible here and would be necessary if for a particular algorithm the output from individual computations was needed. With our device design though we can also construct readout gates that measure the ratio $\langle|\alpha|^2\rangle:\langle|\beta|^2\rangle$ for the qubits passing out of each Q1DC. The brackets indicate an average of the qubit spin components over $\sim 3\times 10^9$ quantum computations per second. Since each computation from each SAW minimum is nominally identical in our scheme, this ratio should be the same as that for the individual qubits exiting from each Q1DC. Such averaging may even compensate for decoherence and errors from random events in a given network. We present three ways for measuring these averages here.

A. Magnetic readout

The simplest readout idea conceptually is to use the spin-valve effect to measure the orientation of each output qubit using ferromagnetic Ohmic contacts.[54] Figure 12 shows a specific design. The two Ohmic contacts are ferromagnetic and have magnetizations pointing in opposite directions so that they have different resistances to the two spin components of incoming qubits. If the total width of these Ohmic contacts is made less that the spin coherence length this

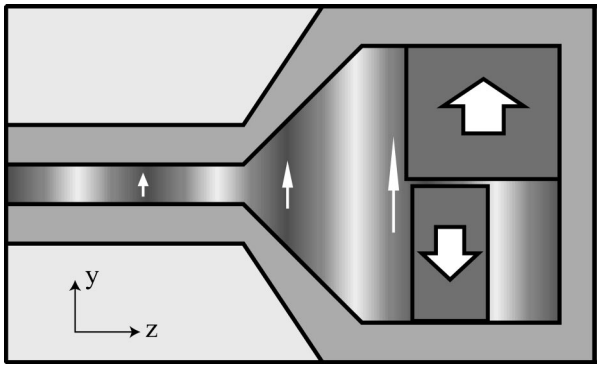

FIG. 12. Schematic diagram showing a readout gate that uses magnetic Ohmic contacts. The Q1DC is defined by two etched trenches and is controlled by 2DEG's above and below. The magnetic Ohmic contacts are placed in a widened part of the Q1DC.

should result in the currents that flow through them to ground reflecting the spin orientation of the output qubits. Such a readout gate could be calibrated using a set of qubits of known orientation. The stray fields that the magnetic contacts produce may be compensated for with single-qubit gates prior to detection.

B. Double occupation readout

Figure 13 shows a readout gate which is an adaptation of the two-qubit gate. It operates by comparing a test qubit (upper channel) with an unknown qubit (lower channel). In the central region there is a gold surface gate to produce an adjustable tunnel barrier between the upper and lower channels. This enables entanglement of incoming qubit wave functions. If the test qubit has the same spin orientation as the unknown qubit then no tunneling will occur between the two channels in the central region and the two incoming electrons will simply pass into Ohmic contacts A and B. However, if they have opposite spin, tunneling can occur and there is a finite probability that the exiting dots will be doubly occupied (see Fig. 8) either in the upper or lower channel. The gate is designed so that if this occurs one of these electrons can further tunnel across a narrow barrier to Ohmic contact C. Thus the ratio of the currents passing into A, B, and C will reflect the spin of the unknown electron relative to that of the known test electron.

C. Stern-Gerlach readout gate

Figure 14 shows a readout gate which is based on the

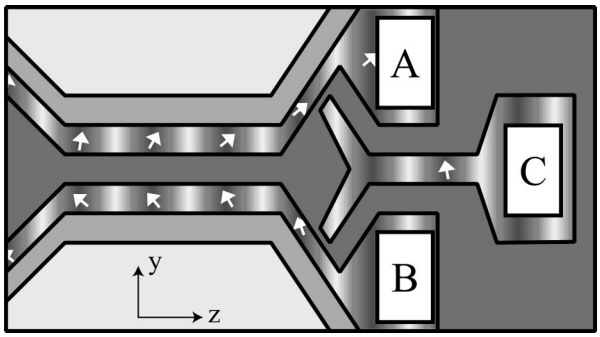

FIG. 13. Schematic diagram showing a readout gate that exploits the possibility of double occupation in a two-qubit operation.

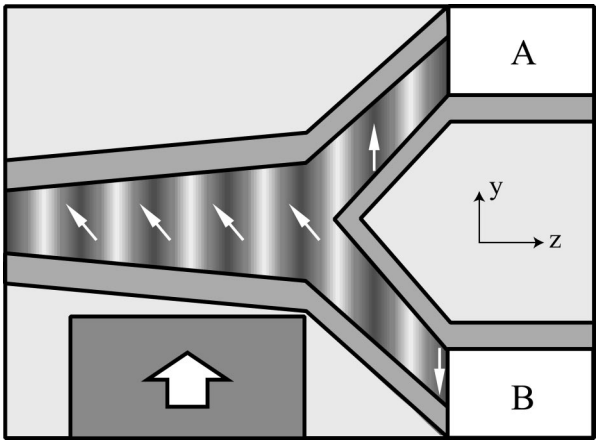

FIG. 14. A schematic diagram showing a readout gate that uses the Stern-Gerlach effect.

Stern-Gerlach effect. The single magnetic gate produces a magnetic field which is spatially varying in the y direction. Through the Zeeman term, this then produces an equal and opposite force F_{SG} on the different spin components of the incoming qubits so that the ratio of the currents flowing into Ohmic contacts A and B should be representative of their spin components along the y direction. Since electrons are charged particles, this readout gate would need to be designed to eliminate, or compensate for, the effect of the Lorentz force F_{Lor}. It is nominally significantly larger $F_{Lor}/F_{SG}=ev_{SAW}B/\frac{1}{2}g\mu_B\partial B_y/\partial y\sim 10^8 B/\partial B_y/\partial y$. The Lorentz force deriving from the magnetic field in the y direction acts in the direction perpendicular to the 2DEG plane, the x direction, and is therefore compensated for by the 2DEG quantum well confinement. The Lorentz force deriving from any resultant component of the magnetic field in the x direction will produce a force in the y direction and will therefore alter the relative currents into A and B. This could be compensated for by introducing a second pole piece and applying a dc bias V_{dc} between them to balance the force: $F=0=E+v_{SAW}B_R$, where $E=V_{dc}/s$ is the electric field between the pole pieces (separation s) and B_R is the resultant magnetic field in the x direction. For a separation between pole pieces of $s=5$ μm a resultant field of $B_R=0.1$ T could be compensated by a dc bias $V_{dc}=1.5$ mV. The device would need to be calibrated by comparing the currents for polarized and unpolarized currents.

VI. ERRORS AND DECOHERENCE

A. Fabrication errors

The SAW quantum-gate network consists of a set of static metal or etched gates. Errors in their patterning will lead to a quantum-gate network performing a different unitary transformation from the one intended.

Errors in the length of magnetic split gates will lead to either an over or an under rotation of spins for single-qubit gates. In principle, this kind of error can be compensated for by splitting the magnetic gates into sections and applying different potential differences between pairs of split gates to move the electrons closer to or further from them and therefore modify the field that they see. Each gate would need to

be individually tuned in this way. For a single gate it would be possible to design it to be sufficiently long so that such fabrication errors were irrelevant, but for a network, such small errors would build up.

For the two-qubit gate the design is such that the length of the tunneling region is not crucial since, by applying a potential to the central metal gate, we have control over its height.

Errors in the width of Q1DC's could lead to double occupation or occupation of complicated linear combinations of orbital states. Such errors can be compensated for by applying suitable biases to surface gates.

If local patterned magnets are used then any design must take account of stray fields that they may introduce into other parts of the system. Either these fields would need to be screened using superconducting surface gates or they would need to be incorporated into the circuit design.

Molecular beam epitaxy (MBE) grown GaAs HEMT structures typically provide a clean system for the study of quantum effects. However, some level of impurities and disorder is inevitable. The presence of this disorder will have a similar effect to channel width variation and could be compensated for in the same way. However, additionally, if a trap state or other impurity is very close to a Q1DC, it could even remove an electron or add an extra electron to a SAW minimum occasionally. Provided the error rate due to these mechanisms was low, it would be removed in the averaging of the readout gates.

Johnson noise on surface gates will cause fluctuations in all gates. The degree of filtering applied to the voltage lines providing the potential to set these gates in an experimental system will have to be limited by the desired operation speed. At 3 GHz, gate potential fluctuations may not be a significant problem, and again such fluctuations will tend to be averaged out in the readout gates.

Temperature effects may cause a severe problem. The SAW single-electron devices require cooling to 1.2 K for optimum operation, but the large powers applied to the transducers to produce the effect will inevitably cause local heating at one end of the device. Whether this will affect device performance will have to be determined experimentally.

Surface-gate patterning would need to be designed such that it did not significantly modify the SAW amplitude through screening. This can be compensated for by using a HEMT with a 2DEG, which is sufficiently deep that surface screening is irrelevant.[48,56]

B. Decoherence

Decoherence is not an intrinsic limiting factor to quantum computation since quantum error correction codes can be used to correct for its effects.[14–19] For our design, implementing these codes would simply result in the necessity to use more C-NOT gates for the same computation.

Semiconductor systems suffer from a large number of possible sources of decoherence. Any coupling between any line of N qubits and any other system of particles could reduce its coherence. The sources of decoherence for our system would include at least: coupling to other lines of N qubits in neighboring SAW minima, and to other electrons, in surface gates, on donor impurities and in the adjacent 2DEG's; piezoelectric coupling to phonon modes; coupling to nuclear spins; and coupling to radio-frequency photons.

The problem with coupling to other lines of qubits could be minimized, or even eliminated, by using SAW transducer designs that produce strong SAW minima at multiples of the fundamental operation frequency, allowing the SAW waveform to be nonsinusoidal. A pulsed mode operation is also possible, by switching the signal to the transducer at radio frequencies. These techniques could be used to separate adjacent SAW minima by distances larger than the SAW wavelength and therefore reduce crosstalk between them.

The problem of decoherence of electrons in a quantum dot caused by interaction with nearby conduction electrons has been demonstrated in transport measurements.[57–60] These measurements indicate that even a weak capacitive coupling to a nearby system can reduce quantum coherence within a device. Avoiding such coupling is a matter of design, but utimately will be an intrinsic limitation to any semiconductor quantum-gate design.

Bulk spin-resonance measurements[61] show that the limiting factor for the spin lifetime in GaAs is phonon scattering. However, even at 5 K, lifetimes of up to 100 ns were found. In this time the SAW travels approximately 300 μm, so given a typical gate size of a micron, it should be possible for a SAW minimum to traverse hundreds of single and two-qubit gates before the computation it is performing loses all coherence.

Decoherence due to acoustic phonons in coupled quantum dots has been investigated experimentally.[62] They find that the tunneling process that occurs in these devices actually produces phonons, thereby reducing the coherence time. Since the two-qubit gate in our scheme relies on tunneling between adjacent quantum dots, this may also prove to be a limitation on our design. However, since the majority of these phonons will be of very long wavelength, it should be possible to reduce their effect by placing the device in a suitable cavity.[62]

The presence of radio frequency photons from the microwave signal used to generate the SAW can be significantly reduced by issolating the device with suitable screening. Since the radio frequency used in experiments with SAW's has a wavelength of approximately 10 cm, a cavity much smaller than this would work well.

If the electron spins couple to the nuclear spins of the host crystal, then this provides an additional mechanism for decoherence. Such coupling has been observed in GaAs systems[63–65] and its effect on double quantum dots has been described theoretically in Ref. 39.

VII. SUMMARY

We have suggested a way in which SAW devices can be used for quantum computation. The idea involves the capture of electrons in pure spin states from a 2DEG by a SAW to form qubits. Single-qubit operations are performed using local magnetic fields produced by magnetic surface gate patterning. Two-qubit operations are performed by allowing exchange coupling between qubits through a controllable tunnel barrier. A quantum computation with one of these devices would consist of a single SAW minimum dragging a line of N qubits through a patterned array of single and two-

qubit gates. Each SAW minimum would perform the same computation. A number of different schemes for reading out the final state of qubits have been proposed: magnetic Ohmic contacts; double occupation in two-qubit gates; and the Stern-Gerlach effect. The major problem problem for this kind of implementation will be decoherence arising from coupling with: other electrons; radio frequency photons; phonons; and nuclear spins. However, these problems are generic to any semiconductor quantum computation proposal and we believe that the repetition (three billion time per second) which our implementation allows could be exploited to counteract these problems.

ACKNOWLEDGMENTS

We are grateful to C. J. B. Ford, D. P. DiVincenzo, D. Loss, G. Milburn, and G. Burkard for instructive discussions and encouragement in this work. CHWB acknowledges an Advanced Fellowship from the EPSRC.

[1] John Preskill Lecture Notes on Quantum Information and Computation available at http://www.theory.caltech.edu/ preskill/ ph229.
[2] *Introduction to Quantum Computation and Information*, edited by Hoi-Kwong Lo, Sandu Popescu, and Tim Spiller (World Scientific, Singapore, 1999).
[3] R.P. Feynmann, Found. Phys. **16**, 507 (1986).
[4] S. Lloyd, Science **273**, 1073 (1996).
[5] C. Zalka, Proc. R. Soc. London, Ser. A **454**, 313 (1998).
[6] S. Somaroo, C.H. Teng, T.F. Havel, R. Laflamme, and D.G. Cory, Phys. Rev. Lett. **82**, 5381 (1999).
[7] P.W. Shor, *Proceedings of 35th Annual IEEE Symposium on Foundations of Computer Science* (IEEE Computer Society Press, Los Alamitos, CA, 1994), p. 124.
[8] L.K. Grover, Phys. Rev. Lett. **79**, 325 (1997).
[9] L.K. Grover, Phys. Rev. Lett. **79**, 4709 (1997).
[10] L.K. Grover, Phys. Rev. Lett. **80**, 4329 (1998).
[11] S. Lloyd, Science **261**, 1569 (1993).
[12] D.P. DiVincenzo, Phys. Rev. A **51**, 1015 (1995).
[13] T. Sleator and H. Weinfurter, Phys. Rev. Lett. **74**, 4087 (1995).
[14] P.W. Shor Phys. Rev. A **52**, 2493 (1995).
[15] A. Stean, Proc. R. Soc. London, Ser. A **452**, 2551 (1996).
[16] I.L. Chuang and Y. Yamamoto, Phys. Rev. A **52**, 3489 (1995).
[17] I.L. Chuang and R. Laflamme, quant-ph/9511003 (unpublished).
[18] I.L. Chuang, R. Laflamme, and J.-P. Paz, quant-ph/9602018 (unpublished).
[19] D.G. Cory, W. Mass, M. Price, E. Knill, R. Laflamme, W.H. Zurek, T.F. Havel, and S.S. Somaroo, Phys. Rev. Lett. **81**, 2152 (1998).
[20] G.J. Milburn, Phys. Rev. Lett. **62**, 2124 (1989).
[21] A. Barenco, D. Deutsch, A. Ekert, and R. Jozsa, Phys. Rev. Lett. **74**, 4083 (1995).
[22] J.I. Cirac and P. Zoller, Phys. Rev. Lett. **74**, 4091 (1995).
[23] T. Pellizari, S.A. Gardiner, J.I. Cirac, and P. Zoller, Phys. Rev. Lett. **75**, 3788 (1995).
[24] Q.A. Turchette, C.J. Hood, W. Lange, H. Mabuchi, and H.J. Kimble, Phys. Rev. Lett. **75**, 4710 (1995).
[25] C. Monroe, D.M. Meekhof, B.E. King, W.M. Itano, and D.J. Wineland, Phys. Rev. Lett. **75**, 4714 (1995).
[26] N.A. Gershenfeld and I.L. Chuang, Science **275**, 350 (1997).
[27] I.L. Chuang, L.M.K. Vandersypen, X. Zhou, D.W. Leung, and S. Lloyd, Nature (London) **393**, 143 (1998).
[28] T.F. Havel, S.S. Somaroo, C.-H. Tseng, and D.G. Cory, quant-ph/9812086 (unpublished).
[29] N.H. Bonadeo, J. Erland, D. Gammon, D. Park, D.S. Katzer, and D.G. Steel, Science **282**, 1473 (1998).
[30] P.M. Platzman and M.I. Dykman, Science **284**, 1967 (1999).
[31] B.E. Kane, Nature (London) **393**, 133 (1998).
[32] R. Vrijen, E. Yablonovitch, K. Wang, H.W. Jiang, A. Balandin, V. Roychowdury, T. Mor, and D. DiVincenzo, quant-ph/9905096 (unpublished).
[33] A. Shnirman, G. Schön, and Z. Hermon, Phys. Rev. Lett. **79**, 2371 (1997).
[34] D.V. Averin, Solid State Commun. **105**, 659 (1998).
[35] L.B. Ioffe, V.B. Geshkenbein, M.V. Feigel'man, A.L. Fauchére, and G. Blatter, Nature (London) **398**, 679 (1999).
[36] Y. Makhlin, G. Schön, and A. Shnirman, Nature (London) **398**, 305 (1999).
[37] Y. Nakamura, Yu.A. Pashkin, and J.S. Tsai, Nature (London) **398**, 786 (1999).
[38] G. Burkard, D. Loss, and D.P. Divincenzo, Phys. Rev. B **59**, 2070 (1999).
[39] D. Loss and D.P. Divincenzo, Phys. Rev. A **57**, 120 (1998).
[40] D. Loss, G. Burkard, and E.V. Sukhorukov, cond-mat/9907133 (unpublished).
[41] J.M. Shilton, V.I. Talyanskii, M. Pepper, D.A. Ritchie, J.E.F. Frost, C.J.B. Ford, C.G. Smith, and G.A.C. Jones, J. Phys.: Condens. Matter **8**, L531 (1996).
[42] V.I. Talyanskii, J.M. Shilton, M Pepper, C.G. Smith, C.J.B. Ford, E.H. Linfield, D.A. Ritchie, and G.A.C. Jones, Phys. Rev. B **56**, 1510 (1997).
[43] V.I. Talyanskii, J.M. Shilton, J. Cunningham, M. Pepper, C.J.B. Ford, C.G. Smith, E.H. Linfield, D.A. Ritchie, and G.A.C. Jones, Physica B **251**, 140 (1998).
[44] R. Ionicioiu, G. Amaratunga, and F. Udrea, quant-ph/9907043 (unpublished).
[45] A. Kristensen, J.B. Jensen, M. Zaffalon, C.B. Sorensen, S.M. Reimann, M. Michel, and A. Forchel, J. Appl. Phys. **83**, 607 (1998).
[46] A. Kristensen, P.E. Lindelof, J.B. Jensen, M. Zaffalon, J. Hollingbery, S.W. Pedersen, J. Nygard, H. Bruus, S.M. Reimann, C.B. Sorensen, M. Michel, and A. Forchel, Physica B **251**, 180 (1998).
[47] J. Cunningham, V.I. Talyanskii, J.M. Shilton, M. Pepper, M.Y. Simmons, and D.A. Ritchie, Phys. Rev. B **60**, 4850 (1999).
[48] G.R. Aizin, G. Gumbs, and M. Pepper, Phys. Rev. B **58**, 10 589 (1998).
[49] P. Maksym (unpublished).
[50] K. Flensberg, Q. Niu, and M. Pustilnik, cond-mat/9908096 (unpublished).
[51] M. Pustilnik, K. Flensberg, and Q. Niu, cond-mat/9909187 (unpublished).
[52] A.M. Robinson and C.H.W. Barnes, *preprint*.
[53] A.G.C. Haubrich, D.A. Wharam, H. Kriegelstein, S. Manus, A.

Lorke, J.P. Kotthaus, and A.C. Gossard, Appl. Phys. Lett. **70**, 3251 (1997).
[54] S. Gardelis, C.G. Smith, C.H.W. Barnes, E.H. Linfield, and D.A. Ritchie, Phys. Rev. B **60**, 7764 (1999).
[55] A. Shnirman and G. Schön, Phys. Rev. B **57**, 15 400 (1998).
[56] M.J. Hoskins and B.J. Hunsinger, J. Appl. Phys. **55**, 413 (1984).
[57] A. Yacoby, M. Heiblum, V. Umansky, H. Shtrikman, and D. Mahalu, Phys. Rev. Lett. **73**, 3149 (1994).
[58] A. Yacoby, M. Heiblum, D. Mahalu, and H. Shtrikman, Phys. Rev. Lett. **74**, 4047 (1995).
[59] A. Yacoby, R. Schuster, and M. Heiblum, Phys. Rev. B **53**, 9583 (1996).
[60] E. Buks, R. Schuster, M. Heiblum, D. Mahalu, and V. Umansky, Nature (London) **391**, 871 (1998).
[61] J.M. Kikkawa and D.D. Awschalom, Phys. Rev. Lett. **80**, 4313 (1998).
[62] T. Fujisawa, T.H. Oosterkamp, W.G. van der Wiel, B.W. Broer, R. Aguado, S. Tarucha, and L.P. Kouwenhoven, Science **282**, 932 (1998).
[63] A. Berg, M. Dobers, R.R. Gerhardts, and K.v. Klitzing, Phys. Rev. Lett. **64**, 2563 (1990).
[64] S. Kronmüller, W. Dietsche, J. Weis, K.v. Klitzing, W. Wegscheider, and M. Bichler, Phys. Rev. Lett. **81**, 2526 (1998).
[65] S. Kronmüller, W. Dietsche, K.v. Klitzing, G. Denninger, W. Wegscheider, and M. Bichler, Phys. Rev. Lett. **82**, 4070 (1999).